Published in final edited form as:
Metabolism. 2013 June ; 62(6): 861–872. doi:10.1016/j.metabol.2012.12.012.

Renin Inhibition and AT_1R blockade improve metabolic signaling, oxidant stress and myocardial tissue remodeling

Adam Whaley-Connell[a,b,c,f,g,i], **Javad Habibi**[a,b,c,g,i], **Nathan Rehmer**[b,c,g], **Sivakumar Ardhanari**[b,c], **Melvin R Hayden**[b,c,g,i], **Lakshmi Pulakat**[a,b,c,e,f,g,i], **Caroline Krueger**[b,c], **Carlos M Ferrario**[j], **Vincent G DeMarco**[a,b,c,g,h,i], and **James R Sowers**[a,b,c,d,g,i]

[a]Harry S. Truman Memorial Veterans Hospital, 800 Hospital Drive, Columbia, MO 65201

[b]University of Missouri-Columbia School of Medicine, One Hospital Drive, Columbia, MO 65212

[c]Department of Internal Medicine, MA415 Medical Sciences Building, One Hospital Drive, Columbia, MO 65212

[d]Department of Medical Pharmacology and Physiology, MA415 Medical Sciences Building, One Hospital Drive, Columbia, MO 65212

[e]Department of Nutrition and Exercise Physiology, 217 Gwynn Hall, Columbia, MO 65211

[f]Division of Nephrology and Hypertension, One Hospital Drive, Columbia, MO 65212

[g]Division of Endocrinology, Diabetes and Metabolism, One Hospital Drive, Columbia, MO 65212

[h]Division of Cardiovascular Medicine, One Hospital Drive, Columbia, MO 65212

[i]Diabetes and Cardiovascular Center, One Hospital Drive, Columbia, MO 65212

[j]Departments of Surgery, Internal Medicine-Nephrology, and Physiology-Pharmacology, Wake Forest University School of Medicine, Medical Center Boulevard, Winston-Salem, NC 27157-1090

Abstract

Objective—Strategies that block angiotensin II actions on its angiotensin type 1 receptor or inhibit actions of aldosterone have been shown to reduce myocardial hypertrophy and interstitial fibrosis in states of insulin resistance. Thereby, we sought to determine if combination of direct renin inhibition with angiotensin type 1 receptor blockade *in vivo*, through greater reductions in

Corresponding author Adam Whaley-Connell, DO, MSPH, Associate Professor of Medicine, Harry S Truman Memorial Veterans Hospital, 800 Hospital Drive, Columbia, MO 65211, Phone: (573)882-2273, Fax: (573)884-5530, whaleyconnella@health.missouri.edu.

The authors have nothing to disclose

Author Contribution: Adam Whaley-Connell and James R. Sowers conceived the studies, planned the experiments, analyzed and interpreted the data, and prepared, edited and finalized the paper. Javad Habibi performed immunofluorescence studies, analyzed and interpreted the data, and edited the paper. Vincent G. DeMarco and Sivakumar Ardhanari and performed the echocardiography studies, analyzed and interpreted the data, and edited the paper. Melvin R. Hayden performed the electron microscopy, interpreted. Nathan Rehmer and Caroline Krueger were responsible for animal husbandry and performance of experiments. Carlos Ferrario provided the Ren2 model and assisted editing and finalizing of the manuscript. Lakshmi Pulakat helped interpret the data, edit and finalize the manuscript.

systolic blood pressure (SBP) and aldosterone would attenuate left ventricular hypertrophy and interstitial fibrosis to a greater extent than either intervention alone.

Materials/Methods—We utilized the transgenic Ren2 rat which manifests increased tissue expression of murine renin which, in turn, results in increased renin-angiotensin system activity, aldosterone secretion and insulin resistance. Ren2 rats were treated with aliskiren, valsartan, the combination (aliskiren+valsartan), or vehicle for 21 days.

Results—Compared to Sprague-Dawley controls, Ren2 rats displayed increased systolic blood pressure, elevated serum aldosterone levels, cardiac tissue hypertrophy, interstitial fibrosis and ultrastructural remodeling. These biochemical and functional alterations were accompanied by increases in the NADPH oxidase subunit Nox2 and 3-nitrotyrosine content along with increases in mammalian target of rapamycin and reductions in protein kinase B phosphorylation. Combination therapy contributed to greater reductions in systolic blood pressure and serum aldosterone but did not result in greater improvement in metabolic signaling or markers of oxidative stress, fibrosis or hypertrophy beyond either intervention alone.

Conclusions—Thereby, our data suggest that the greater impact of combination therapy on reductions in aldosterone does not translate into greater reductions in myocardial fibrosis or hypertrophy in this transgenic model of tissue renin overexpression.

Keywords

Direct Renin Inhibition; Angiotensin II Type 1 receptor; Echocardiography; Ren2 rat

Introduction

Pharmacologic intervention targeting renin-angiotensin-aldosterone system (RAAS) interruption has been shown to slow progression of heart failure [1,2]. However, these anti-hypertensive strategies only attenuate heart failure morbidity and mortality across trials which suggest a significant remaining amount of residual risk for heart disease [3,4]. In this context, activation of the RAAS contributes to maladaptive left ventricular (LV) remodeling through promotion of oxidative stress and inflammation, processes that contribute to hypertrophy and fibrosis in the progression of heart failure [1,5,6]. Combination treatment strategies that block of the actions of angiotensin II (Ang II) on its angiotensin type 1 receptor (AT1R) (ARBs) or inhibit actions of aldosterone though antagonism of the mineralocorticoid receptor (MR) have been shown to reduce LV hypertrophy and interstitial fibrosis.

It is acknowledged that activation of the AT_1R, as well as the MR, in cardiomyocytes and cardiac fibroblasts leads to increased generation of excess reactive oxygen species (ROS), in part, by a NADPH oxidase-dependent pathway [7–11]. In cardiomyocytes, both AngII and aldosterone regulate growth pathways such as mammalian target of rapamycin (mTOR) signaling as well as increasing generation of ROS [7,9,12,13]. Further, both hormones have been shown to reduce insulin metabolic signaling, in part, by decreased downstream protein kinase B/Akt phosphorylation/activation. The cumulative effect of these hormones contributes to myocardial maladaptive remodeling, fibrosis, and hypertrophy. The role of NADPH oxidase activation and generation of ROS in cardiac pathology is underscored by the fact that NADPH oxidase inhibitors and free radical scavengers, as well as AT_1R blockade and MR antagonism, attenuate these adverse effects [7–9,11,14–19].

Many hypertensive patients treated with an ARB exhibit a phenomenon known as “aldosterone breakthrough” [20]. Aldosterone breakthrough is likely due, in part, to increases in tissue renin and the activity of non-angiotensin-converting(ACE) enzymes that

cleave Ang I to form Ang II which eventually leads to increased synthesis and release of aldosterone. As renin activation is a pivotal step in generation of Ang II and downstream aldosterone secretion, there has been increased interest in exploring the utility of combination renin inhibition with AT_1R blockade as an attractive therapeutic target to prevent myocardial tissue injury and heart failure through targeting greater reductions in aldosterone [21,22].

Recent work from our group and others suggests that combination RAAS blockade would improve blood pressure responses compared to individual components [23,24]. However, the greater reduction in systolic blood pressure (SBP) did not lead to improvements in proteinuria or indices of kidney injury [23]. As preclinical data would support aldosterone contributes to a reactive myocardial fibrosis [11,25,26] and Ang II contributes to mechanisms of myocardial hypertrophy [11,25–28] both through generation of oxidant stress independent of changes in blood pressure, we hypothesized that combination therapy with *in vivo* direct renin inhibition and AT_1R blockade would then attenuate myocardial tissue hypertrophy and interstitial fibrosis to a greater extent than either intervention alone. We further hypothesized this would occur through greater reductions in aldosterone that would lead to greater attenuation of insulin metabolic pathways and cardiac tissue oxidative stress. Work done in a model of enhanced RAAS activation and insulin resistance, the transgenic TG(mRen2)27 rat (Ren2) that has the murine renin transgene expressed in various tissues including the adrenal, suggests that adrenal glomerulosa production of aldosterone is partly tissue renin dependent and that direct adrenal renin inhibition may attenuate aldosterone production [29]. Due to relative species specificity for only human and mouse renin, renin inhibition with aliskiren cannot be studied effectively in conventional rat models [30,31]. To circumvent this issue, we have employed the transgenic Ren2 which harbors both the native Ren2 and the murine renin transgene, with increased tissue Ang II, circulating aldosterone and insulin resistance [32]. Thereby, use of the transgenic Ren2 rat allows for investigation of the role that combination of direct renin inhibition with AT_1R blockade compared to the individual interventions will have on myocardial tissue injury.

Methods

Animals and Treatments

All animal procedures were approved by the University of Missouri animal care and use committees and housed in accordance with NIH guidelines. Using a prevention paradigm to target development of hypertrophy and fibrosis, young Ren2 rats (6–9 weeks of age) and age-matched Sprague-Dawley (SD) littermates were randomly assigned to sham-treated (R2-C and SD-C, respectively; n=6 each), aliskiren-treated (R2-A; n=6 each) at 50mg/kg/day, valsartan treated (R2-V; n=5) at 30 mg/kg/day, or a combination of aliskiren and valsartan (R2-A+V; n=6) in saline via intraperitoneal injection for 21 days. Aliskiren was provided by Novartis Research Laboratories and prepared fresh daily in sterile 0.9% normal saline. Dosing was based on previous studies in Ren2 rats [23,30,33].

Systolic blood pressure (SBP) and Aldosterone

Restraint conditioning was initiated before blood pressure measurements were performed as previously described [23,32,33]. SBP was measured in triplicate on separate occasions throughout the day using the tail-cuff method (Harvard Systems, Student Oscillometric Recorder) prior to initiation of treatment and on days 19 or 20 prior to sacrifice at 21 days. Serum aldosterone was measured at the end of the treatment period via by radioimmunoassay using a double antibody assay at the Vanderbilt Hormone & Analytic Service Core Laboratory at the Vanderbilt Diabetes Research and Training Center [23].

Echocardiography

Transthoracic echocardiography, was performed on isoflurane anesthetized rats using a GE Vivid i system with an 11.5-MHz phased-array pediatric probe [34,35]. 2D echocardiograms in the apical long and parasternal short axis views and M-mode examination at the level of LV mid-cavity were performed. LV septal and posterior wall thicknesses (SWT and PWT respectively) and LV internal diameter were measured both at end diastole and end systole (LVIDd and LVIDs respectively). Fractional shortening (FS) and ejection fraction (EF) were calculated according to the formulas %FS = [(LVIDd - LVIDs)/LVIDd]×100; and %EF = [stroke volume/LV volume at end diastole]×100, respectively. Relative wall thickness (RWT) was calculated according to the formula RWT = (SWTd + PWTd)/LVIDd. All parameters were assessed by using an average of three beats, and calculations were made in accordance with the American Society of Echocardiography guidelines as well as specific guidelines for rodent echocardiography[34,35]. All data were acquired and analyzed by a single blinded observer using Echo PAC (GE Vingmed) offline processing.

Immunohistochemistry

Harvested heart tissues were prepared as previously described [23,32,33]. Briefly, non-specific binding sites on rehydrated paraffin embedded sections were blocked in 5% BSA, 5% donkey serum and 0.01% sodium azide in HEPES buffer for four hours in a humidity chamber. Following a brief rinse, sections were incubated with 1:100 goat anti-Nox2 (Santa Cruz), 1:50 goat polyclonal serine (Ser)^{2448}phosphorylated (p)-mTOR (BD, Inc) in 10-fold diluted blocking agent overnight. After washing, sections were incubated for four hours with 1:300 Alexa-fluor donkey anti-goat 647 for Nox2 and (p)-mTOR (Invitrogen). The slides were examined under a bi-photon confocal microscope, and the images were captured with LSM imaging system. Signal intensities were analyzed with MetaVue.

3-Nitrotyrosine (3-NT)Immunostaining

3-NT was quantified as previously described [23,32,33]. Briefly, tissue sections were incubated overnight with 1:200 primary rabbit polyclonal anti-3-NTantibody (Millipore). Sections were then washed and incubated 30 min with secondary antibodies, biotinylated link, and streptavidin-HRP. After several rinses with distilled water, diaminobenzidine was applied for 12 min, and sections were again rinsed and stained with hematoxylin for 45 sec, rehydrated, and mounted with a permanent media. The slides were viewed under a bright field (Nikon 50i) microscope and 40× images captured with a snap *cf* camera.

Cardiomyocyte Hypertrophy

To evaluate cardiomyocyte hypertrophy,4 μm of paraffin embedded heart sections were incubated with 1:50 heme-pomatia agglutinin (HPA) conjugated to Alexa fluor 647 for four hours. Then, two fluorescent confocal images were captured from each cross. On each image the area of the 20 cardiomyocytes were measured by MetaVue or Metamorph. The average size of all measured cardiomyocytes within a sample was determined and expressed in units of cross sectional area (μm^2).

Myocardial Fibrosis

Additional four μm thick sections were cut and mounted on glass slides and stained with Verhoeff van Gieson (VVG) stain, which stains collagen fibers pink, to evaluate interstitial fibrosis as previously described [23,32,33]. The relative amount of collagen within 10 representative regions was determined by MetaVue, and an average value recorded for each LV sample was expressed as arbitrary units. Samples from five rats from each of the five treatment groups were analyzed.

Ultrastructural Observations with Transmission Electron Microscopy (TEM)

Heart tissue was thinly sliced, placed immediately in primary TEM fixative, and prepared as previously described [23,32,33]. A JOEL 1400 TEM microscope (JOEL Ltd, Tokyo, Japan) was utilized to view all samples.

Western Blots

Heart protein was quantified using BCA assay (Pierce, Rockford, IL). Laemmli buffer was added to the lysates and equal amounts were loaded onto Criterion gels 7.5%. Blots were blocked in 1%BSA in 1XTBST for one hour and incubated O/N at 4°C with rabbit monoclonalanti-Akt antibody (Epitomics Inc, CA). Bands were visualized with ECL on a Biorad Phosphorimager and quantified with Image Lab software (Biorad, Hercules, CA). For Akt, the NuPage large protein analysis system was used (Invitrogen, Grand Island, NY). Briefly, lysates were prepared for loading on to Novex 3–8% Tris-Acetate gels using sample buffer and reducing agent supplied with the kit. Proteins were transferred for ~18 hours at 15V at 4°C. Blots were blocked as above and anti-Akt antibody was added for overnight incubation at 4°C.

Statistical Analysis

All values are expressed as mean±standard error. Statistical analyses were performed using ANOVA with Tukey's post hoc test for all other outcomes (Sigma Stat 3.1, Systat Software Inc., Chicago, IL).

Results

Combination therapy lowers SBP and aldosterone more than individual therapy in the transgenic Ren2 rat

There were increases in SBP in the Ren2 (214±6 mm Hg) compared to SD controls (143±4 mm Hg; $p<0.05$); findings improved with administration of both aliskiren(159±13 mm Hg) and valsartan (147±5 mm Hg, respectively; each $p<0.05$). There were greater reductions in SBP in the Ren2 with combination treatment (126±4 mm Hg; $p<0.05$) compared to treatment with either aliskiren or valsartan alone. Similar to our observation with SBP, there were increases in circulating serum aldosterone levels in the Ren2 (319±4 pg/ml) compared to SD controls (255±4 pg/ml, $p<0.05$) and administration of both aliskiren and valsartan reduced serum aldosterone (233±28 and 268±42 pg/ml, respectively; each $p<0.05$). Additionally, there were greater reductions with combination treatment(77±10 pg/ml, $p<0.05$) compared to treatment with either aliskiren or valsartan alone in the Ren2 rats.

Combination adds little to improvements in hypertrophy on echocardiography in the Ren2

There were no changes in systolic indices (EF) in either strain or with treatment as determined by 2D echocardiography (Fig 1). However, there were observable increases in measures of thickness (e.g. septal, posterior and relative wall) in the Ren2 compared to SD controls. There were similar improvements in echo indices of LV thickness between aliskiren, valsartan or combination treatment in the Ren2.

In evaluation of LV function, the LV internal diameter in diastole was not different among the groups (data not presented). However the internal dimension in systole was greater in Ren2 compared to SD controls. Despite these differences in the internal dimensions, there is no significant difference in LVEF or FS among the groups. Dimensions of the left atrium and aorta were not different statistically.

Combination adds little to improvements in hypertrophy and fibrosis in the Ren2

Increases in LV mass are associated with cardiomyocyte size[5,10]. Our data suggest that consistent with increases in wall thickness, there are increases in cardiomyocyte size as determined by HPA in Ren2 compared to SD controls (Fig 2A).HPA is a N-acetylgalactosamine (GalNAc) binding lectin specific for cell-surface ligand binding and is useful to clearly demarcate cell-cell borders. The increases in cardiomyocyte size in the Ren2 were improved to a similar extent between aliskiren, valsartan, and combination treatment.

The development of interstitial fibrosis contributes significantly to LV hypertrophy. Commensurate with our findings of SWT, LV weight, and myocyte size in the Ren2 compared to SD controls there were increases in LV interstitial fibrosis (Fig 2B), findings improved to a similar extent between aliskiren, valsartan, and combination treatment.

On ultrastructural analysis utilizing TEM, there was organized fibrillar collagen in the interstitial perivascular regions of the Ren2 (Fig 2C) compared to SD control wherein there is usually loose areolar collagen in the interstitium. In the valsartan treated Ren2 rats there was loose areolar collagen, with no organized collagen present similar to SD controls and there were no areas of organized collagen with aliskiren and combination treatment.

Combination adds little to improvements in oxidative stress and Ser kinases in the Ren2

Increases in cardiac mass and sustained overload contribute to contractile dysfunction and heart failure through poorly understood mechanisms. Data implicates oxidant stress in myocardial tissue hypertrophy and fibrosis through engagement of redox-sensitive kinases. In this regard, the increases in LV thickness, myocyte size, and fibrosis occurred in parallel with increases in the NADPH oxidase subunit Nox2 and 3-NTstaining in the Ren2 compared to SD controls (Fig 3A and B), findings improved to a similar extent between aliskiren, valsartan, and combination treatment.

Recent work highlights several redox-sensitive pathways such as mTOR and protein kinase B(Akt) signaling systems that regulate growth and metabolism[12,13,36,37]. In this regard, there were increases in Ser^{2448}(p)-mTOR and reductions in Ser^{473}(p)-Akt in the Ren2 compared to SD controls (Fig 4A and B, respectively), findings that were either decreased or increased, respectively, to a similar extent over three weeks with administration of aliskiren, valsartan, and the combination. Since increased (p) of mTOR and decreased (p) of Akt are associated with reduced insulin metabolic signaling [1,5] this suggest that combination therapy did not improve this metabolic signaling in the hearts of insulin resistant Ren2 rats [25,32,33].

Combination adds little to improvements in ultrastructural remodeling in the Ren2

On ultrastructural analysis in cross section, there were excessive numbers of mitochondria in the Ren2 compared to SD controls, which appear to morphologically compress the sarcoplasmic reticulum structures as previously observed [25] (Fig 5). The mitochondria cristae were often absent and typically the mitochondria matrix is lost and appears more electron-lucent. Notably, there was also thinning and disorganization of sarcomeres. The Ren2 also displayed elongation of the intercalated disc compared to SD controls (Fig 6). This resulted in the appearance of duplication. These mitochondria abnormalities and duplication of the intercalated disc are improved to a similar extent between aliskiren, valsartan, and combination treatment.

Discussion

Our current data support the concept that interruption of the RAAS with direct renin inhibition, AT_1R blockade and both interventions in combination, comparably improve mechanisms that relate tometabolic signaling, myocardial tissue fibrosis and hypertrophy under conditions of RAAS activation in the transgenic Ren2 rat. Our work extend prior observations that combination led to greater improvements in blood pressure in the congenic mRen2. Lewis to [24] yet, improved Akt (p)/activation and reduced (p) of mTOR, oxidant markers (e.g Nox2 and 3-NT), interstitial fibrosis, LV hypertrophy and cardiomyocyte size, and tissue remodeling to a similar extent as either component. Our recent data further corroborate findings that combination treatment led to greater reductions in SBP as well as aldosterone levels compared to either intervention alone [23]. However, contrary to our hypothesis combination therapy provided little additional benefit compared to either intervention alone in improving markers of myocardial tissue fibrosis, metabolic signaling and hypertrophy. Thereby our data highlight the notion that Ang II-dependent tissue responses to changes in blood pressure predominate over the potential impact of reductions in aldosterone on markers of myocardial tissue fibrosis, metabolic signaling and hypertrophyin this insulin resistant transgenic model.

Our finding that combination therapy led to greater reductions in aldosterone corroborates data from a human cohort in sodium-replete subjects [37]. Considering the importance of MR-dependent signaling for heart tissue fibrosis and remodeling, we had hypothesized the combination strategy would provide greater cardio-protection in this model due to greater reductions in aldosterone. However, the lack of additional reductions in fibrosis and hypertrophy in the combination arm, despite the additional reductions in SBP and aldosterone, may signal a detrimental response for combination therapy on growth and proliferative responses and warrant future mechanistic investigation. This future mechanistic work could potentially help understand observations from a recent human cohort the ALTITUDE trial which was stopped prematurely due to an increase in cardiovascular events in the combination arm utilizing aliskiren with an ACE inhibitor or ARB [38].

The presence of LV hypertrophy is a significant predictor of cardiovascular outcomes and heart failure, and therapies targeting the RAAS have been demonstrated to improve LV hypertrophy. Hemodynamic (ventricular overload and coronary perfusion pressure) or humoral factors (Ang II, insulin, and aldosterone)regulate the development of hypertrophy [3,22,34]. Although, it is thought the primary stimulus for hypertrophy is mechanical stress due to hemodynamic overload and elevations in systolic pressure over time. In the Ren2 model, the RAAS is activated by elevations in tissue Ang II as well as circulating aldosterone. Further, direct renin inhibition, AT_1R blockade and MR antagonism have been shown to improve interstitial fibrosis and hypertrophy in this model [18,25,33]. Thereby, our observation that LV thickness, cardiomyocyte hypertrophy, and ultrastructural remodeling were improved to a similar extent among the treatments groups suggests the hemodynamic (BP) response to treatment trumped the benefit of the additional reduction in aldosterone in this transgenic model [23].

In regards to the impact of changes in blood pressure on fibrosis, previous work suggest MR-dependent fibrosis can occurin the hypertrophied LV as well as in the non-hypertrophied LV under conditions of a normal work load [39–41]. Myocardial and peri-coronary fibroblasts that synthesize collagens which promotes myocardial tissue fibrosis have been demonstrated to possess MRs [25,39]. The LV of transgenic Ren2 rats exhibited interstitial fibrosis in addition to increases in LV thickness and myocyte size and renin inhibition as well as blockade of the AT_1R improved measures of fibrosis and hypertrophy [18,25,33,40,41]. Our additional observation that combination led to no greater reductions in

fibrosis suggest that mechanism to promote fibroblasts in this model are more dependent on hemodynamic that hormonal factors, per se. Thereby, our findings are contrary to the premise that greater reductions in aldosterone would then lead to greater reductions in fibrosis in this transgenic model and corroborate recent work in Ang II infused mice suggesting that fibroblast migration and interstitial fibrosis may be pressor-dependent processes[42].

Despite this pressor-dependent fibrotic response uncovered in the current investigation, *ex vivo* and *in vitro* studies support the notion that Ang II and aldosterone facilitate fibrosis and hypertrophy, in part, through the increases in ROS under conditions of overload [40]. Indeed, hypertrophic LV of the Ren2 exhibited enhanced NADPH oxidase driven oxidative stress as indicated by elevations in Nox2 and consequent3-NT levels. These findings corroborate previous work in this model, and they suggest an autocrine/paracrine role for the RAS in the myocardium leading to high tissue levels of Ang II and generation of NADPH oxidase-derived ROS[18,32,33,43]. Similar to hypertrophy and fibrosis indices, Nox2 and 3-NT were normalized between the three treatment groups further corroborating recent work which suggests that changes in NADPH oxidase is strain or load dependent [39–43].

Recent data support a role for AT_1R signaling in promotion of fibrosis in coronary smooth muscle cells and hypertrophy in cardiac tissue through activation of the mTOR [44,45]. In cardiomyocytes, blockade of the AT_1R reduces mTOR signaling and cell size and improves insulin metabolic signaling, in part, by targeting pathways that lead to reductions in NADPH oxidase subunits. In this regard, cell growth is redox dependent and recent data from HEK-392 cells suggest mTOR, similar to other kinases, is redox-sensitive where in oxidizing agents diamide or phenylarsine oxide increased downstream target S6K [44–46]. While activation of mTOR has not been shown to be strain or load dependent in the heart, the observed reductions in Ser^{2448} p-mTOR with direct renin inhibition, AT_1R blockade and in combination corroborate that engagement of mTOR is, in part, Ang II dependent.

It should be noted that mTOR contains a phosphatidylinositol-3-kinase (PI3-K) like domain and is considered a substrate for Akt activity. Further, Ser^{2448} serves as an Akt target for mTOR in LV remodeling under conditions of ischemia-reperfusion [12]. However, recent work supports that mTOR engages a mechanism to regulate insulin receptor substrate-1 (IRS-1) expression and thereby insulin-dependent engagement of PI3-K/Akt under conditions of RAAS activation, causing tissue and systemic insulin resistance[13,47]. In this context, selective mTORC1 inhibition can elicit increased Ser^{473} (p) of Akt through IRS-1, alternatively mTOR activation has been shown to attenuate Ser^{473} p-Akt through suppression of IRS-1. This reciprocal relationship between mTOR and Akt activation is consistent with the notion that site-specific (p) can dictate the transport, proliferative, or growth dependent responses under varying experiment conditions. The reduction in heart p-Akt is consistent with previous literature on alterations in tissue and systemic insulin sensitivity in the Ren2 manifesting RAAS activation [18,48].

In summary, results from the current investigation indicate that either renin inhibition or AT_1R blockade, whether alone or in combination, improved to a similar extent LV pro-fibrotic and growth factors, oxidative stress and associated interstitial fibrosis, and hypertrophy. Despite the fact that combination therapy provided an additional benefit in SBP and aldosterone reduction beyond what was observed in SD controls, this did not translate to further reductions in markers of myocardial tissue fibrosis, oxidative stress and hypertrophy. Thereby, our data highlight that Ang II-dependent changes in blood pressure and tissue responses predominate over the potential impact of reductions in aldosterone on markers of myocardial tissue hypertrophy and fibrosis in this transgenic model.

It should be noted in our finding that treatment with the individual components in the Ren2 led to improvements comparable to controls suggesting that combination of the two might not be relevant in the study design of this model. Additionally, as both renin inhibition and AT_1R blockade completely prevented a hypertrophic or fibrotic response in the Ren2, the addition of a combitorial strategy with this dosing strategy confounded any expectation of interpretation of a synergistic reduction. Thereby, dosing strategies to evaluate combinatorial blood pressure lowering effects of the agents over a time course might yield important inferences in this model and other physiological relevant models that display activation of the RAAS. In addition, future work directed at exploring other combinatorial strategies such as AT_1R blockade or renin inhibition with antagonism of the MR need exploration [49–51].

Acknowledgments

The authors would like to acknowledge the technical contributions of Mona Garro as well as students Safwan Hyder and Bennett Krueger. The authors wish to thank Brenda Hunter for her assistance in preparing the manuscript.

Funding: This research was supported by the NIH HL-73101 and NIH HL-107910 to JRS, and AG040638 to AWC, and HL-051952 to CMF. There was also support from the Veterans Affairs Merit System (0018) for JRS as well as CDA-2 BB47 to AWC and the ASN-ASP Junior Development Grant in Geriatric Nephrology to AWC supported by a T. Franklin Williams Scholarship Award; Funding provided by: Atlantic Philanthropies, Inc, the John A. Hartford Foundation, the Association of Specialty Professors, and the American Society of Nephrology. This research was also supported by Novartis Corporation.

Abbreviations

Angt II	angiotensin II
ACE	angiotensin-converting enzyme
AT_1R	Ang II type 1 receptor
EF	ejection fraction
FS	fractional shortening
HPA	heme-pomatia agglutinin
LV	left ventricular
LVID	LV internal diameter
mTOR	mammalian target of rapamycin
MR	mineralocorticoid receptor
GalNAc	N-acetylgalactosamine
PWT	posterior wall thicknesses
ROS	reactive oxygen species
RWT	relative wall thickness
RAS	renin-angiotensin system
RAAS	renin-angiotensin-aldosterone system
SWT	septal wall thicknesses
SD	sprague-dawley
SBP	systolic blood pressure

3-NT	3-nitrotyrosine
Ren2	transgenic TG(mRen2)27 rat
VVG	Verhoeff van Gieson

References

1. Sowers JR, Whaley-Connell A, Epstein M. The emerging clinical implications of the role of aldosterone in the metabolic syndrome and resistant hypertension. Ann Intern Med. 2009; 150:776–783. [PubMed: 19487712]
2. Botdorf J, Chaudhary K, Whaley-Connell A. Hypertension in cardiovascular and kidney disease. Cardiorenal Med. 2011; 1:183–192. [PubMed: 22096454]
3. Reinhard H, Hansen PR, Wiinberg N, et al. NT-proBNP, echocardiographic abnormalities and subclinical coronary artery disease in high risk type 2 diabetic patients. Cardiovasc Diabetol. 2012; 11:19–19. [PubMed: 22390472]
4. Parving HH, Brenner BM, McMurray JJ, et al. Aliskiren Trial in Type 2 Diabetes Using Cardio-Renal Endpoints (ALTITUDE): rationale and study design. Nephrol Dial Transplant. 2009; 2009; 24:1663–1671. [PubMed: 19145003]
5. Pulakat L, Demarco VG, Whaley-Connell A, et al. The impact of over-nutrition on insulin metabolic signaling in the heart and the kidney. Cardiorenal Med. 2011; 1(2):102–112. [PubMed: 22258397]
6. Baker KM, Chernin MI, Wixson SK, et al. Renin-angiotensin system involvement in pressure-overload cardiac hypertrophy in rats. A. J Physiol. 1990; 259:H324–H332.
7. Bendall JK, Cave AC, Heymes C, et al. Pivotal role of a gp91(phox)-containing NADPH oxidase in angiotensin II-induced cardiac hypertrophy in mice. Circulation. 2002; 105:293–296. [PubMed: 11804982]
8. Malhotra R, Sadoshima J, Brosius FC, et al. Mechanical stretch and angiotensin II differentially upregulate the renin-angiotensin system in cardiac myocytes in vitro. Circ Res. 1999; 85:137–146. [PubMed: 10417395]
9. Sadoshima J, Izumo S. Molecular characterization of angiotensin II-induced hypertrophy of cardiac myocytes and hyperplasia of cardiac fibroblasts. Critical role of the AT1 receptor subtype. Circ Res. 1993; 73:413–423. [PubMed: 8348686]
10. Sadoshima J, Xu Y, Slayter HS, et al. Autocrine release of angiotensin II mediates stretch-induced hypertrophy of cardiac myocytes in vitro. Cell. 1993; 75:977–984. [PubMed: 8252633]
11. Sun Y, Zhang J, Lu L, et al. Aldosterone-induced inflammation in the rat heart : role of oxidative stress. Am J Pathol. 2002; 161:1773–1781. [PubMed: 12414524]
12. Clemente CF, Xavier-Neto J, Dalla Costa AP, et al. Focal adhesion kinase governs cardiac concentric hypertrophic growth by activating the AKT and mTOR pathways. J Mol Cell Cardiol. 2012; 52:493–501. [PubMed: 22056317]
13. Shiojima I, Yefremashvili M, Luo Z, et al. Akt signaling mediates postnatal heart growth in response to insulin and nutritional status. J Biol Chem. 2002; 277:37670–37677. [PubMed: 12163490]
14. Elmedal B, de Dam MY, Mulvany MJ, et al. The superoxide dismutase mimetic, tempol, blunts right ventricular hypertrophy in chronic hypoxic rats. Br J Pharmacol. 2004; 141:105–113. [PubMed: 14656807]
15. Harrison DG, Cai H, Landmesser U, et al. Interactions of angiotensin II with NAD(P)H oxidase, oxidant stress and cardiovascular disease. J Renin Angiotensin Aldosterone Syst. 2003; 4:51–61. [PubMed: 12806586]
16. Privratsky JR, Wold LE, Sowers JR, et al. AT1 blockade prevents glucose-induced cardiac dysfunction in ventricular myocytes: role of the AT1 receptor and NADPH oxidase. Hypertension. 2003; 42:206–212. [PubMed: 12847113]
17. Tokuda K, Kai H, Kuwahara F, et al. Pressure-independent effects of angiotensin II on hypertensive myocardial fibrosis. Hypertension. 2004; 43:499–503. [PubMed: 14699000]

18. Whaley-Connell A, Govindarajan G, Habibi J, et al. Angiotensin II-mediated oxidative stress promotes myocardial tissue remodeling in the transgenic (mRen2) 27 Ren2 rat. Am J Physiol Endocrinol Metab. 2007; 293:E355–E363. [PubMed: 17440033]
19. Wang H, Shimosawa T, Matsui H, et al. Paradoxical mineralocorticoid receptor activation and left ventricular diastolic dysfunction under high oxidative stress conditions. J Hypertens. 2008; 26:1453–1462. [PubMed: 18551023]
20. Bomback AS, Klemmer PJ. The incidence and implications of aldosterone breakthrough. Nat Clin Pract Nephrol. 2007; 3:486–492. [PubMed: 17717561]
21. Hollenberg NK, Fisher ND, Price DA. Pathways for angiotensin II generation in intact human tissue: evidence from comparative pharmacological interruption of the renin system. Hypertension. 1998; 32:387–392. [PubMed: 9740600]
22. Azizi M, Ménard J, Bissery A, et al. Hormonal and hemodynamic effects of aliskiren and valsartan and their combination in sodium-replete normotensive individuals. Clin J Am Soc Nephrol. 2007; 2:947–955. [PubMed: 17702736]
23. Whaley-Connell AT, Habibi J, Nistala R, et al. Combination direct renin inhibition with angiotensin type 1 receptor blockade improves aldosterone but does not improve kidney injury in the transgenic Ren2 rat. Reg Peptides. 2012; 176:36–44.
24. Moniwa N, Varagic J, Ahmad S, et al. Restoration of the blood pressure circadian rhythm by direct renininhibition and blockade of angiotensin II receptors in mRen2.Lewis hypertensive rats. Ther Adv Cardiovasc Dis. 2012; 6:15–29. [PubMed: 22222314]
25. Stas S, Whaley-Connell A, Habibi J, et al. Mineralocorticoid receptor blockade attenuates chronic overexpression of the renin-angiotensin-aldosterone system stimulation of reduced nicotinamide adenine dinucleotide phosphate oxidase and cardiac remodeling. Endocrinology. 2007; 148:3773–3780. [PubMed: 17494996]
26. Johar S, Cave AC, Narayanapanicker A, et al. Aldosterone mediates angiotensin II-induced interstitial cardiac fibrosis via a Nox2-containing NADPH oxidase. FASEB J. 2006; 20:1546–1548. [PubMed: 16720735]
27. Keidar S, Kaplan M, Pavlotzky E, et al. Aldosterone administration to mice stimulates macrophage NADPH oxidase and increases atherosclerosis development: a possible role for angiotensin-converting enzyme and the receptors for angiotensin II and aldosterone. Circulation. 2004; 109:2213–2220. [PubMed: 15123520]
28. Rocha R, Martin-Berger CL, Yang P, et al. Selective aldosterone blockade prevents angiotensin II/salt-induced vascular inflammation in the rat heart. Endocrinology. 2002; 143:4828–4836. [PubMed: 12446610]
29. Yamaguchi T, Tokita Y, Franco-Saenz R, et al. Zonal distribution and regulation of adrenal renin in a transgenic model of hypertension in the rat. Endocrinology. 1992; 131:1955–1962. [PubMed: 1396339]
30. Feldman DL, Jin L, Xuan H, et al. Effects of aliskiren on blood pressure, albuminuria, and (pro)renin receptor expression in diabetic TG(mRen-2)27 rats. Hypertension. 2008; 52:130–136. [PubMed: 18490518]
31. Nguyen G, Danser AHJ. Prorenin and (pro)renin receptor: a review of available data from in vitro studies and experimental models in rodents. Exp Physiol. 2008; 93:557–563. [PubMed: 18376005]
32. DeMarco VG, Johnson MS, Habibi J, et al. Comparative analysis of telmisartan and olmesartan on cardiac function in the transgenic (mRen2)27 rat. Am J Physiol Heart Circ Physiol. 2011; 300:H181–H1890. [PubMed: 21057043]
33. Whaley-Connell A, Habibi J, Cooper SA, et al. Effect of renin inhibition and AT_1R blockade on myocardial remodeling in the transgenic Ren2 rat. Am J Physiol Endocrinol Metab. 2008; 295:E103–E109. [PubMed: 18460596]
34. Quinones MA, Otto CM, Stoddard M, et al. Recommendations for quantification of doppler echocardiography: A report from the doppler quantification task force of the nomenclature and standards committee of the american society of echocardiography. J Am Soc Echocardiogr. 2002; 15:167–184. [PubMed: 11836492]
35. Hoit BD. Echocardiographic characterization of the cardiovascular phenotype in rodent models. Toxicol Pathol. 2006; 34:105–110. [PubMed: 16507551]

36. Sarbassov DD, Guertin DA, Ali SM, et al. Phosphorylation and regulation of Akt/PKB by the rictor–mTOR complex. Science. 2005; 307:1098–1101. [PubMed: 15718470]
37. Sarbassov DD, Sabatini DM. Redox regulation of the nutrient-sensitive raptor-mTOR pathway and complex. J Biol Chem. 2005; 280:39505–39509. [PubMed: 16183647]
38. [accessed 12-2-12] http://www.novartis.com/newsroom/media-releases/en/2011/1572562.shtml
39. Brilla CG, Zhou G, Matsubara L, et al. Collagen metabolism in cultured adult rat cardiac fibroblasts: response to angiotensin II and aldosterone. J Mol Cell Cardiol. 1994; 26:809–820. [PubMed: 7966349]
40. Sawyer DB, Siwik DA, Xiao L, et al. Role of oxidative stress in myocardial hypertrophy and failure. J Mol Cell Cardiol. 2002; 34:379–388. [PubMed: 11991728]
41. Wang H, Shimosawa T, Matsui H, et al. Paradoxical mineralocorticoid receptor activation and left ventricular diastolic dysfunction under high oxidative stress conditions. J Hypertens. 2008; 26:1453–1462. [PubMed: 18551023]
42. Rosin NL, Sopel M, Falkenham A, et al. Myocardial migration by fibroblast progenitor cells is blood pressure dependent in a model of AngII myocardial fibrosis. Hypertens Res. 2012; 35:449–456. [PubMed: 22258030]
43. Flesch M, Schiffer F, Zolk O, et al. Contractile systolic and diastolic dysfunction in renin-induced hypertensive cardiomyopathy. Hypertension. 1997; 30:383–391. [PubMed: 9314421]
44. Diniz GP, Carneiro-Ramos MS, Barreto-Chaves ML. Angiotensin type 1 receptor mediates thyroid hormone-induced cardiomyocyte hypertrophy through the Akt/GSK-3beta/mTOR signaling pathway. Basic Res Cardiol. 2009; 104:653–667. [PubMed: 19588183]
45. Hafizi S, Wang X, Chester AH, et al. Ang II activates effectors of mTOR via PI3-K signaling in human coronary smooth muscle cells. Am J Physiol Heart Circ Physiol. 2004; 287:H1232–H1238. [PubMed: 15317677]
46. Ohnishi H, Kobayashi H, Okazawa H, et al. Redox regulation of the nutrient-sensitive raptor-mTOR pathway and complex. J Bio Chem. 2004; 279:39505–39509. [PubMed: 15265858]
47. Shi Y, Yan H, Frost P, et al. Mammalian target of rapamycin inhibitors activate the AKT kinase in multiple myeloma cells by up-regulating the insulin-like growth factor receptor/insulin receptor substrate-1/phosphatidylinositol 3-kinase cascade. Mol Cancer Ther. 2005; 4:1533–1540. [PubMed: 16227402]
48. Xu J, Carretero OA, Liao TD, et al. Local angiotensin II aggravates cardiac remodeling in hypertension. Am J Physiol Heart Circ Physiol. 2010; 299:H1328–H1338. [PubMed: 20833959]
49. Yoshiyama M, Omura T, Yoshikawa J. Additive improvement of left ventricular remodeling by aldosterone receptor blockade with eplerenone and angiotensin II type 1 receptor antagonist in rats with myocardial infarction. Nihon Yakurigaku Zasshi. 2004; 124:83–89. [PubMed: 15277726]
50. Fraccarollo D, Galuppo P, Hildemann S, et al. Additive improvement of left ventricular remodeling and neurohormonal activation by aldosterone receptor blockade with eplerenone and ACE inhibition in rats with myocardial infarction. J Am Coll Cardiol. 2003; 42:1666–1673. [PubMed: 14607457]
51. Fraccarollo D, Galuppo P, Schmidt I, et al. Additive amelioration of left ventricular remodeling and molecular alterations by combined aldosterone and angiotensin receptor blockade after myocardial infarction. Cardiovasc Res. 2005; 67:97–105. [PubMed: 15949473]

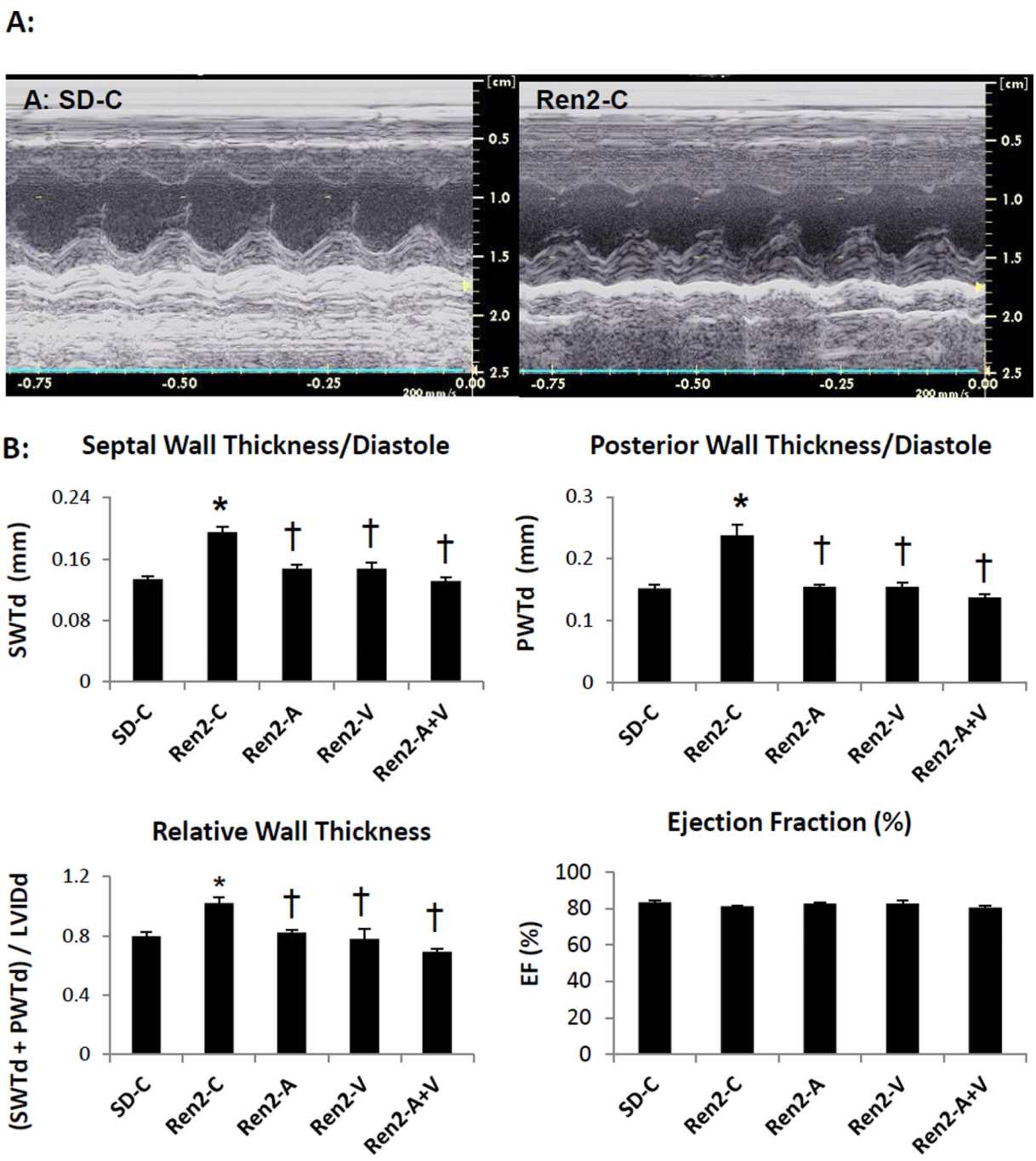

Figure 1. Echocardiography measures in the Ren2 Rat

A) Representative images of m-mode echocardiography of Ren2 controls (Ren2-C) compared to age-matched Sprague-Dawley controls (SD-C) with **B)** LV wall dimensional and ejection fraction measures below. Values presented as mean ± standard error. *, $p<0.05$ when Ren2-C are compared to SD-C; †, $p<0.05$ when Ren2 rats treated with either aliskiren (Ren2-A), valsartan (Ren2-V), or combination (Ren2-A+V) are compared to age-matched Ren2-C.

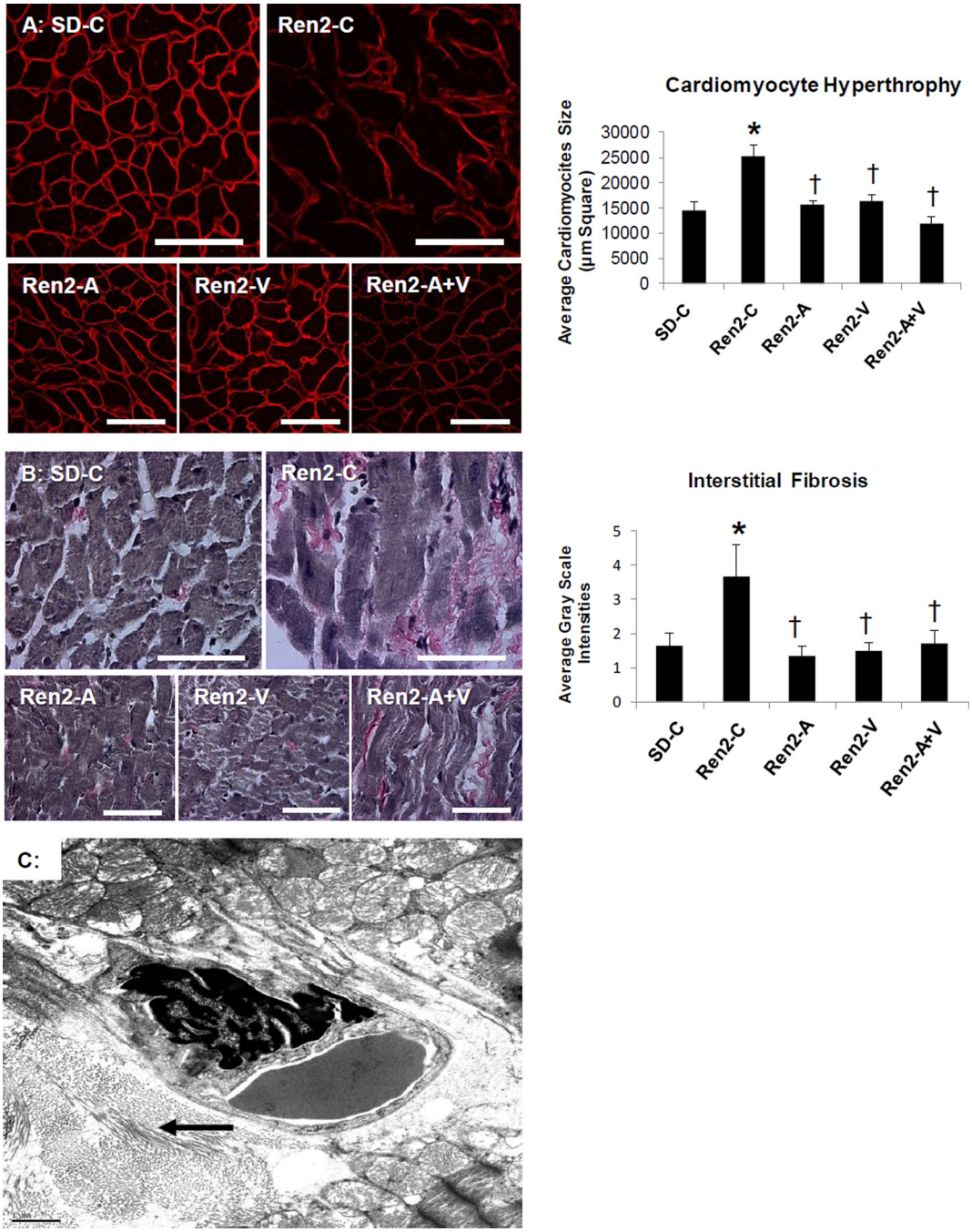

Figure 2. Markers of cardiac tissue hypertrophy and fibrosis in the Ren2 Rat

A) Representative images of semi-quantitative analysis of heme-pomatia agglutinin with measured to the right. **B)** Verhoeff-Van Gieson (VVG) stain for elastin and collagen with measures of tubulointerstitial fibrosis to the right. Values presented as mean ± standard error. *, $p<0.05$ when Ren2 controls (Ren2-C) are compared to age-matched Sprague-Dawley controls (SD-C); †, $p<0.05$ when Ren2 rats treated with either aliskiren (Ren2-A), valsartan (Ren2-V), or combination (Ren2-A+V) are compared to age-matched Ren2-C. **C)** Ultrastructural analysis utilizing transmission electron microscopy of the Ren2 demonstrate organized fibrillar collagen in the interstitial and perivascular regions. This image

demonstrates the marked pericapillary interstitial organized fibrillar collagen (arrow) typical of early ultrastructural fibrosis that appears asteroid-like shaped around a 4×6 μm interstitial capillary. Scale bar = 1 μm.

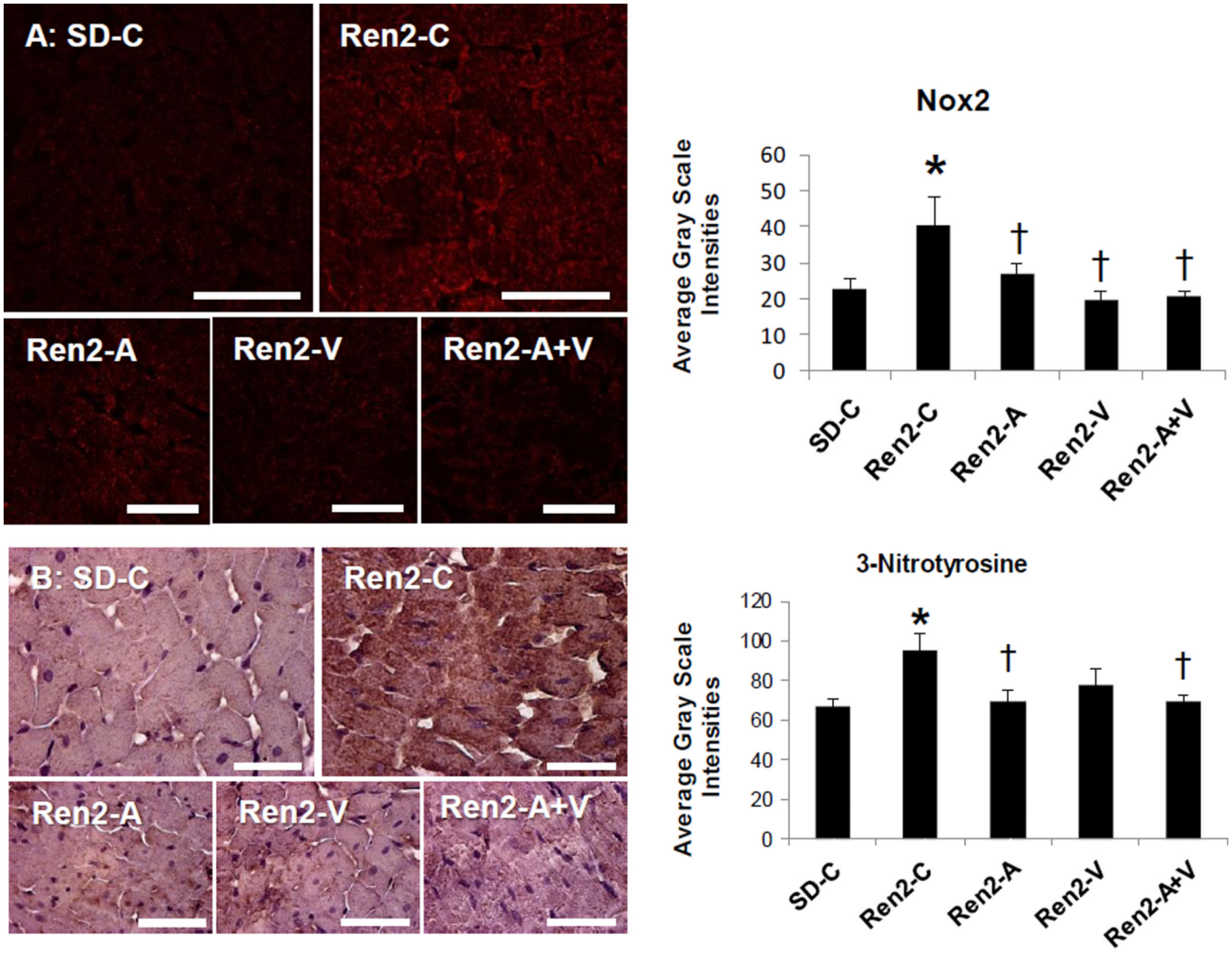

Figure 3. Markers of oxidant stress in the Ren2 Rat

A) Representative confocal images of NADPH oxidase subunit Nox2 with measures of average grey scale intensities to the right. **B)** Representative images of 3-nitrotrysoine with corresponding measures to the right. Values presented as mean ± standard error. *, $p<0.05$ when Ren2 controls (Ren2-C) are compared to age-matched Sprague-Dawley controls (SD-C); †, $p<0.05$ when Ren2 rats treated with either aliskiren (Ren2-A), valsartan (Ren2-V), or combination (Ren2-A+V) are compared to age-matched Ren2-C. Scale bar = 50 μm.

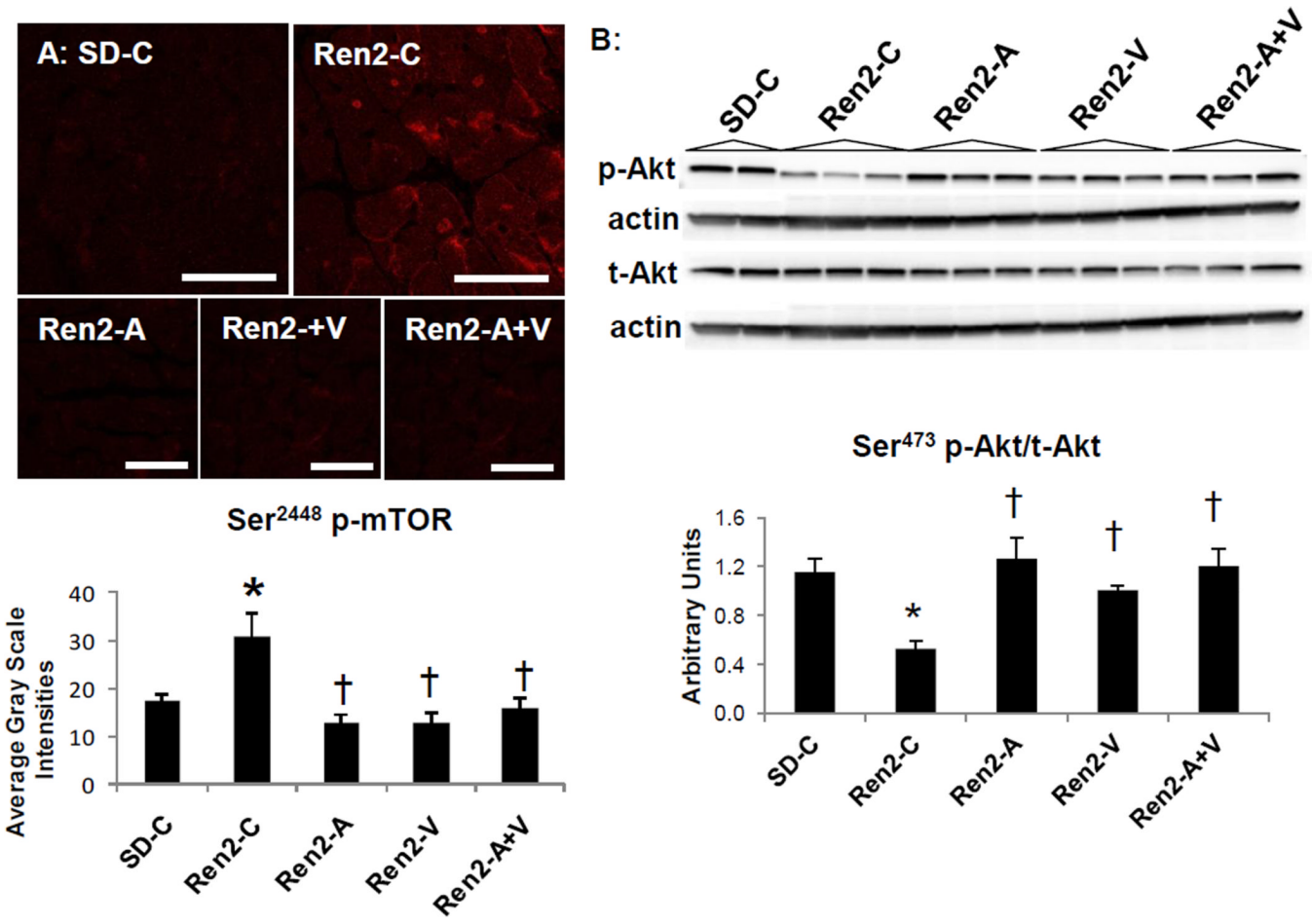

Figure 4. Kinases in cardiac growth in the Ren2 rat

A) Representative images from immunohistochemistry analysis of Serine (Ser) p-mTOR at 2248 with corresponding measures below. Scale bar = 50 μm. **B)** Western blot analysis of phosphorylated (p) Akt at Threonine (Thr) 389 compared to total Akt in cytosolic fractions with densitometry analysis of pAkt/tAkt below. Values presented as mean ± standard error. *, $p<0.05$ when Ren2 controls (Ren2-C) are compared to age-matched Sprague-Dawley controls (SD-C); †, $p<0.05$ when Ren2 rats treated with either aliskiren (Ren2-A), valsartan (Ren2-V), or combination (Ren2-A+V) are compared to age-matched Ren2-C.

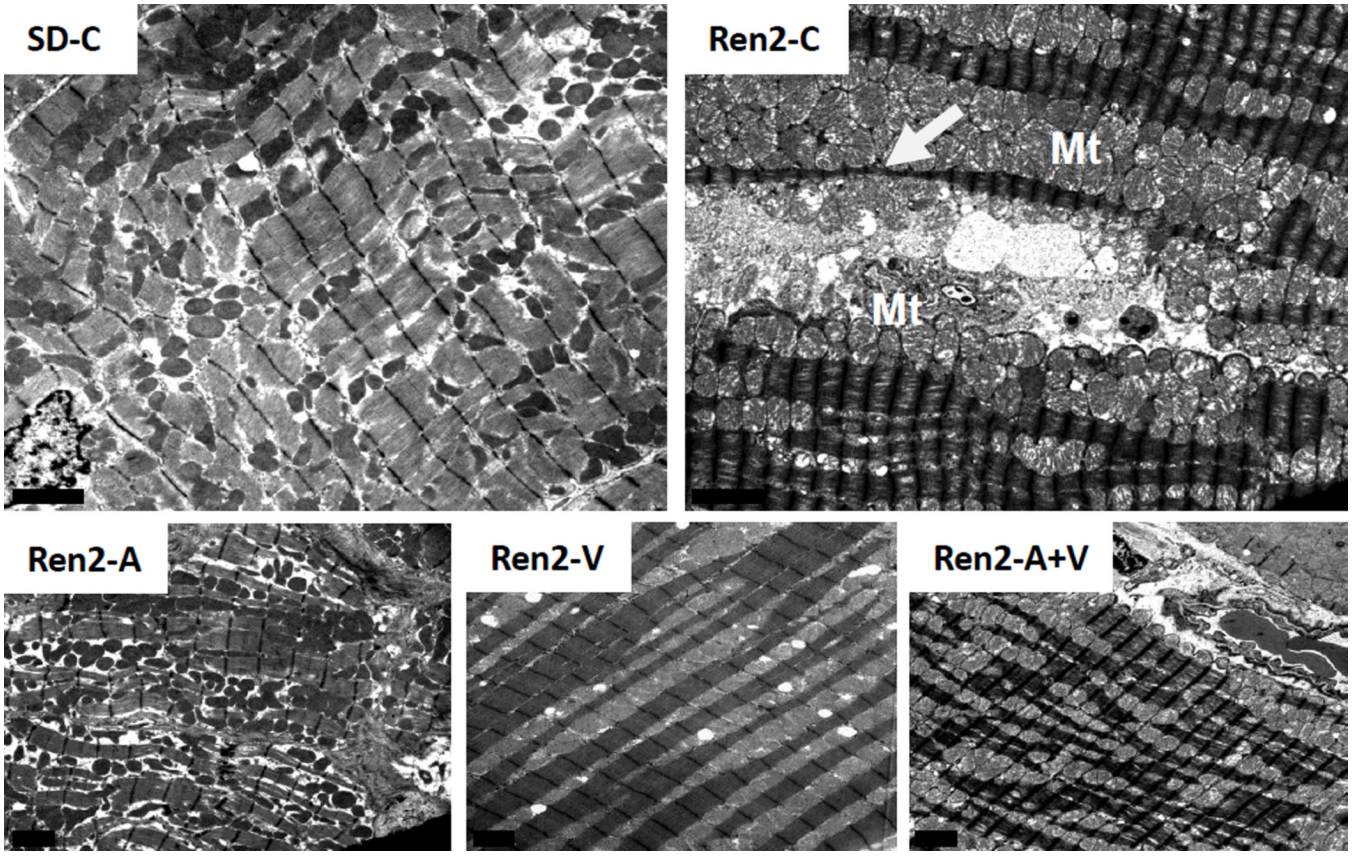

Figure 5. Mitochondrial Content in the Ren2 Heart

Representative images from ultrastructural analysis of the Ren2 myocardium utilizing transmission electron microsopy. In cross section of control transgenic Ren2 rats (Ren2-C; top right panel), there are excessive numbers of mitochondria (Mt) which appear to morphologically compress the sarcoplasmic reticulum (SR) structures (white arrow). The cristae are often absent and typically the mitochondria matrix is lost and appears more electron lucent. Notably, there is also thinning and disorganization of sarcomeres. These observations are not observed in Sprague Dawley control (SD-C) rats and restored in treated Ren2 rats to similar extent with aliskiren (Ren2-A), valsartan (Ren2-V), and combination treatment with both aliskiren and valsartan (Ren2-A+V). Scale bar = 2 μm.

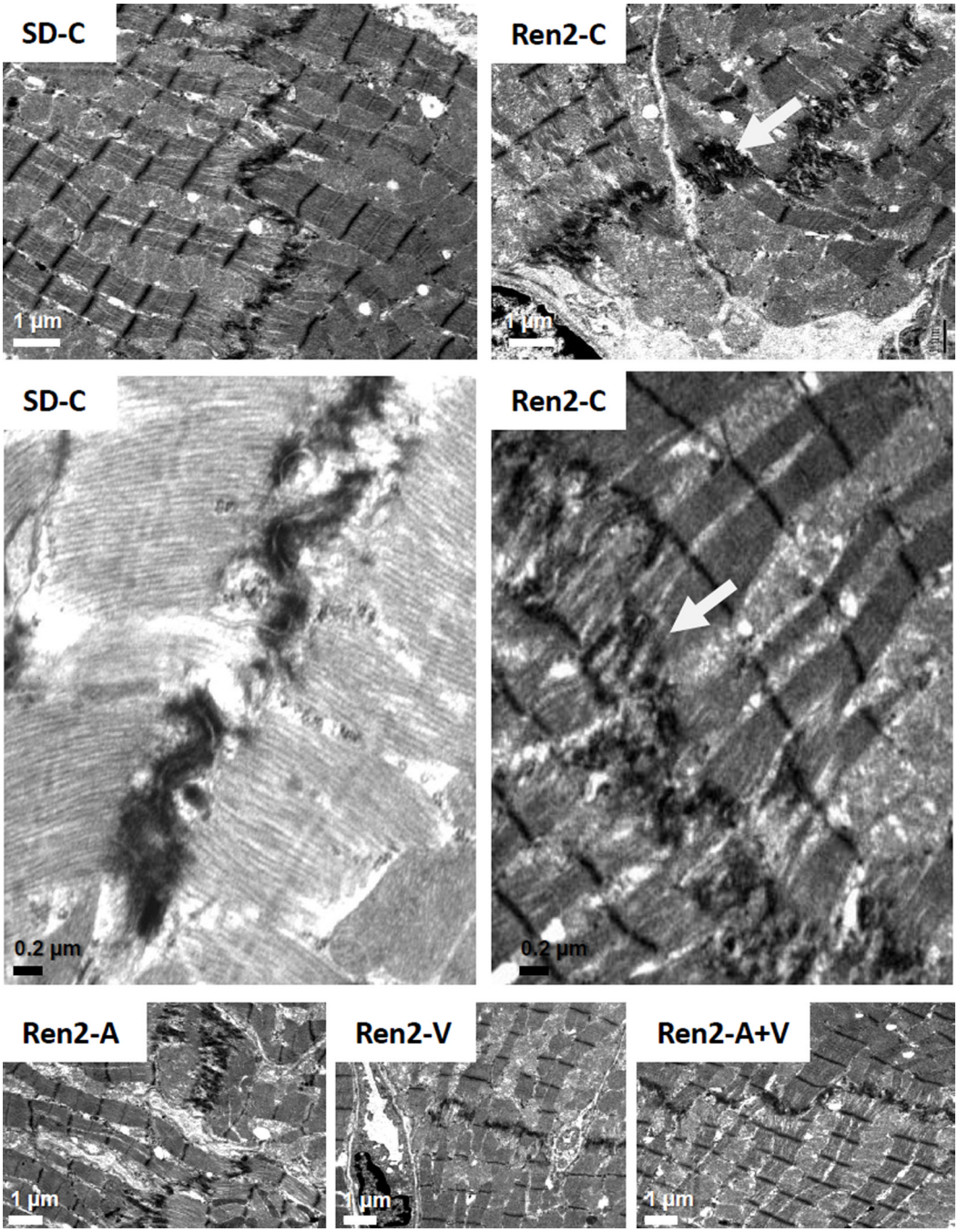

Figure 6. Myocardial tissue remodeling in the Ren2 Heart

Representative images from ultrastructural analysis of the Ren2 myocardium utilizing transmission electron microscopy. In cross section of control transgenic Ren2 rats (Ren2-C; top right panel), the intercalated discs appear to be elongated with increased convolutions in order to increase surface areas between two cardiomyocytes (white arrow). Scale bar = 1 µm. This results in the appearance of being duplicated (middle panels). Scale bar = 0.2 µm. These observations are not observed in Sprague Dawley control (SD-C) rats and restored in treated Ren2 rats to similar extent with aliskiren (Ren2-A), valsartan (Ren2-V), and combination treatment.